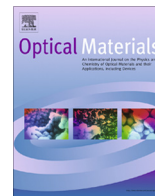




Contents lists available at ScienceDirect

Optical Materials

journal homepage: www.elsevier.com/locate/optmat

Growth and characterization of large size ADP single crystals and the effect of glycine on their growth and properties

P. Rajesh*, P. Ramasamy

Centre for Crystal Growth, SSN College of Engineering, Kalavakkam 603 110, India

ARTICLE INFO

Article history:

Received 15 October 2014

Received in revised form 15 December 2014

Accepted 17 December 2014

Available online xxxx

Keywords:

X-ray diffraction

Growth from solutions

Single crystal growth

Optical materials

ABSTRACT

$80 \times 50 \times 50 \text{ mm}^3$ size 1 mol% of glycine added ADP single crystals have been grown by ACRT technique. The grown crystals have been subjected to powder XRD, FTIR, UV–Vis, HRXRD, TG/DTA, microhardness, laser damage threshold, piezoelectric, dielectric and SHG studies. The crystallinity and the functional groups are confirmed by powder XRD and FTIR spectroscopy. Good transparency in the entire visible region which is an essential requirement for a nonlinear optical crystal is observed for the grown crystals. The structural perfection of the grown crystal has been analyzed by high resolution X-ray diffraction rocking curve measurements. Compared to pure ADP crystal higher hardness was observed from the Vickers hardness studies. Shift in the decomposition temperature has been observed from TG/DTA. Dielectric constant and dielectric loss were measured for the grown crystals for different frequencies and temperatures. Significant piezoelectric charge coefficient has been noted for the glycine doped crystals. Laser damage threshold value has been determined using Nd:YAG laser. Powder SHG measurements show the suitability of the ingot for nonlinear optical applications.

© 2014 Elsevier B.V. All rights reserved.

1. Introduction

Nonlinear optical crystals with high conversion efficiencies of the second, third and fourth harmonics generation, transparent within a broad spectral range are required for numerous applications. In particular KDP and ADP crystals are widely used for frequency conversion and optical switching in modern optoelectronics and photonics. Moreover, these crystals are successfully used as a model system for studying the mechanism of crystal growth from the solution, as well as for finding out a relation between NLO properties and the crystal structure. Unremitting interest to KDP type crystals is caused by their unique physical properties and high manufacturability. In particular, ADP and KDP crystals which possess extremely high optical and structural perfection make it possible to produce elements for doubling and tripling of laser radiation frequency, electro-optic switches and modulators with an aperture of several tens and hundreds of square centimeters to be used, e.g. in laser fusion facilities [1–6]. Zaitseva et al. of LLNL grew large-scale (40–55 cm) KDP crystals at rates of 10–20 mm/d, the rapid growth method is based on the use of “point seed” [7].

In the field of nonlinear optical crystal growth, amino acids are playing a vital role. Many numbers of natural amino acids are

individually exhibiting the nonlinear optical effect. Complex of amino acids are promising material for optical second harmonic generation. The demand for large-size ADP and KDP-type single crystals has increased sharply in recent years because these crystals have important piezoelectric, ferroelectric, electro-optic and nonlinear optical properties [8–10]. Such demand requires the rapid growth of crystals in a shorter duration of time while maintaining the quality and size. In parallel to the invention of new NLO materials, it is also important to modify the physical, optical, and electrical properties of these materials either by adding functional groups or incorporation of dopants for tailor made applications. In the presence of dopants growth promoting factors like growth rate and many of the useful physical properties like optical transparency, second harmonic generation (SHG) efficiency, laser damage threshold (LDT), etc., get enhanced. The dopants or additives also influence the crystalline perfection which may in turn influence the physical properties depending on the degree of doping and as per the accommodating capability of the host crystal. Keeping this in our mind, in our laboratory it was proposed to grow ADP crystal added with 1 mol% of glycine. Glycine, the simplest amino acid, has three polymeric crystalline forms: α , β and γ . Both α and β forms crystallize in centrosymmetric space group P2₁/c. γ -glycine crystallizes in non-centrosymmetric space group P31 making it a candidate for piezo-electric and NLO applications [11].

In this work, we have presented the growth, structural, optical, thermal, mechanical, dielectric and SHG efficiency of glycine doped

* Corresponding author. Tel.: +91 9840522490; fax: +91 44 27475166.

E-mail addresses: rajeshp@ssn.edu.in, rajeshppraj@gmail.com (P. Rajesh).

ADP single crystals grown by slow cooling method. The effects of impurity atoms on the quality and performance of the crystals are analyzed. The results of the doped ADP crystals are compared with the results of the pure ADP crystals.

2. Experimental procedure

2.1. Solubility

ADP is purified by several times of recrystallization in deionized water. The resistivity of the used deionized water is 18 M Ω -cm. The solubility of pure ADP in deionized water was reported by us [12]. In order to know the effect of glycine in solubility of ADP, the 1 mol% of glycine is dissolved fully in 100 ml deionized water and the solubility of ADP is gravimetrically analyzed using the solution. Comparing the result with the pure ADP it is found that the addition of glycine has decreased the solubility of the pure ADP. Similar results have been reported by us in ammonium acetate added ADP [12]. The solubility curve is shown in Fig. 1.

2.2. Crystal growth

The crystal growth has been carried out using slow cooling method. The starting material was ADP pure reagents (G.R., Merck). Pure water by Milli-Q ultrapure water purification system with resistivity of 18.2 M Ω -cm was used as the solvent. Glycine (G.R., Merck) was used as dopant. All experiments are carried out in a standard glass 5000 ml crystallizer, used for conventional crystal growth by the method of temperature reduction. The temperature of crystallizer is controlled using an external water bath, and the temperature fluctuations are less than ± 0.01 °C. The reversible rotation rate of the platform with the crystal was about 35 rpm. The solutions with 1 mol% glycine are filtered through filters with a pore diameter of 0.15 μ m to remove extraneous solid and colloidal particles. After filtration the solutions were overheated at 65 °C. Then the temperature of solution was reduced to 5 °C higher than saturation point and then the seed was Z-cut (one is point seed and one is large crystal plate) placed into the solutions. The temperature was reduced to a critical value of super cooling and the seed crystal began to grow upwards. The grown crystals are shown in Fig. 2.

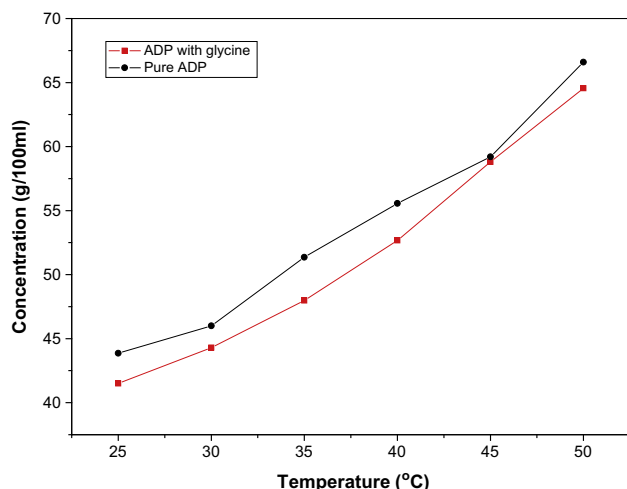


Fig. 1. Solubility of pure and 1 mol% of glycine doped ADP.

3. Characterization

3.1. UV–Vis spectroscopy

Crystal plates of pure and 1 mol% of glycine doped ADP were cut and polished at face (100) without any coating for optical measurements. In both the pure and doped ADP crystals the dimensions of the used crystals are $10 \times 10 \times 5$ mm³. Optical transmission spectra were recorded for the crystals in the wavelength region from 200 to 1100 nm using Perkin–Elmer Lambda 35 UV–Vis spectrometer. The recorded UV–Vis spectra are shown in Fig. 3.

It is observed from the figure that the 1 mol% of glycine doped ADP shows 75% of transmittance. In order to confirm the reproducibility, several times the beam was passed through the various regions of the crystals and the same results were observed. The pure ADP has 65% transmittance [12–14]. The large transmission in the entire visible region enables it to be a good candidate for electro-optic and NLO applications [15]. ADP and KDP crystals grown from deuterium show more than 80% of transparency in

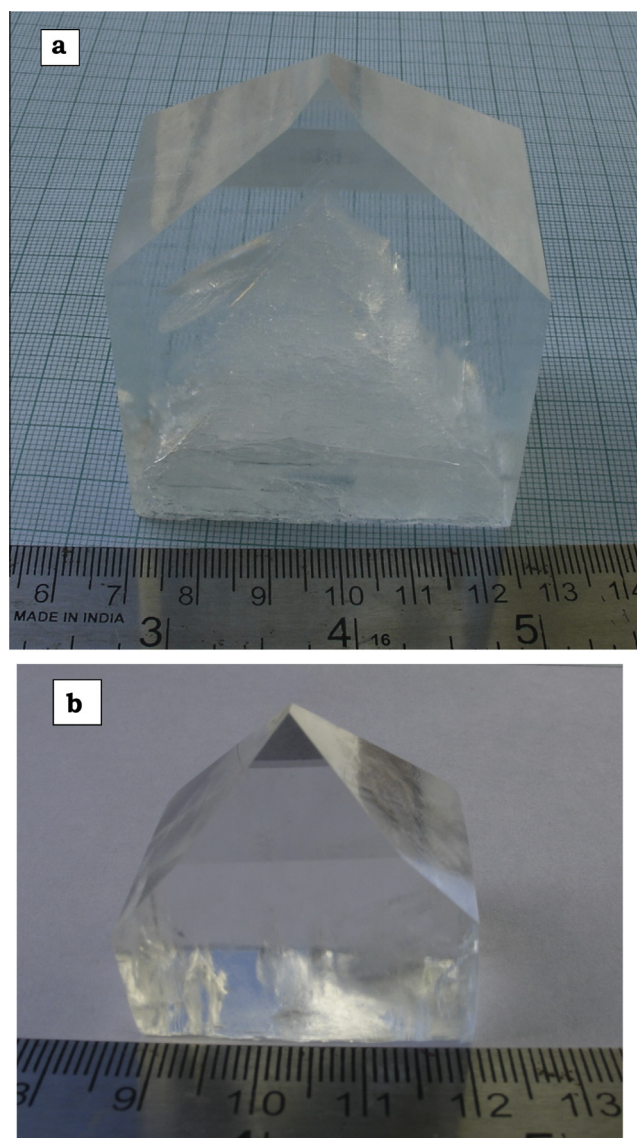


Fig. 2. 1 mol% of glycine doped ADP crystal grown by slow cooling along with seed rotation method using (a) big seed and (b) point seed.

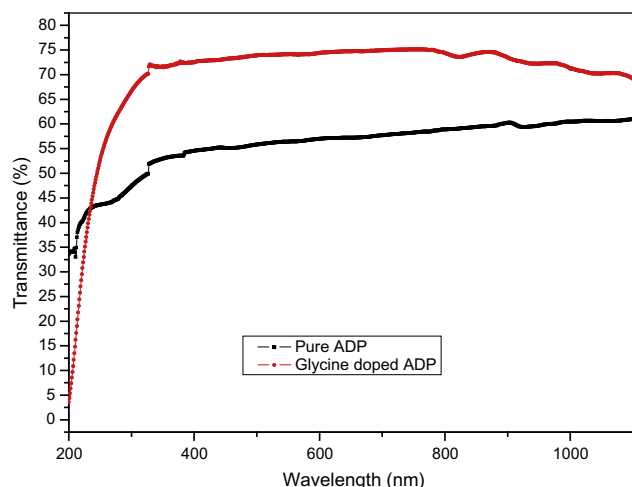


Fig. 3. UV-Vis. spectra of grown crystals.

the entire visible region [3,4]. The grown 1 mol% glycine doped ADP crystal by slow cooling method also shows approximately same transparency and indicates that the crystal has higher crystalline perfection and is suitable for device fabrications. The above results indicate that the addition of glycine increased the transmittance.

3.2. FT-IR spectroscopy

The functional groups of doped ADP have been identified by FT-IR spectroscopy. The FT-IR spectra were recorded using GASCO FT-IR 410 spectrometer in the range $400\text{--}4000\text{ cm}^{-1}$ by the KBr pellet technique. The recorded FT-IR spectrum is shown in Fig. 4. Broad band envelope between 3700 cm^{-1} and 2500 cm^{-1} includes O–H stretching vibrations of ADP. The hydrogen bonding within the crystal is suggested to be the cause for the broadening of the peak. The change in the vibrations between 1600 cm^{-1} and 1100 cm^{-1} in the spectrum of glycine doped ADP indicates the presence of glycine in the lattice of the ADP. The peaks below the 1200 cm^{-1} are due to the PO_4 vibrations and give their peaks at 546 and 462 cm^{-1} . Thus the presence of glycine in the lattice of ADP is established by the FT-IR analysis.

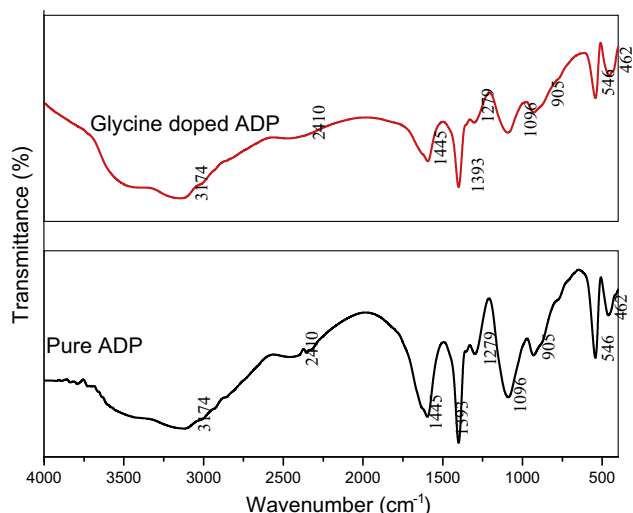


Fig. 4. FTIR spectrum of the grown crystal.

3.3. Powder X-ray diffraction analysis

The X-ray powder diffraction analysis was used to confirm the physical phase of the product. Grown crystals were ground using a porcelain mortar and pestle in order to determine the crystal phases by X-ray diffraction (XRD). Powder X-ray diffraction studies were carried out using Rich Seifert X-ray diffractometer employing $\text{Cu K}\alpha$ (1.54058 \AA) radiation, scanning angle ranging from 10° to 50° at a scan rate $1^\circ/\text{min}$ to study the crystallinity of the grown crystal. It is known from the powder XRD that the obtained diffracted peaks are same with pure ADP crystal. The observed prominent peak of pure and doped ADP is (200), but the intensities of the diffracted peaks are found to be varied. The XRD spectra of pure and doped crystals are shown in Fig. 5. The observed values are in good agreement with the reported values [16].

3.4. HRXRD analysis

Fig. 6 shows the high-resolution rocking/diffraction curve (DC) recorded for a typical ADP + Glycine crystal using (200) diffracting planes in symmetrical Bragg geometry by employing the multi-crystal X-ray diffractometer with $\text{Mo K}\alpha_1$ radiation. As seen in the figure, the DC contains a single peak and indicates that the specimen is free from structural grain boundaries. The FWHM (full width at half maximum) of the curve is 34 arc s which is somewhat more than that expected from the plane wave theory of dynamical X-ray diffraction [17], for an ideally perfect crystal but close to that expected for nearly perfect real life crystals. This much broadness with good scattered intensity along both the wings of the DC indicates that the crystal contains both vacancy and interstitial type of defects [18]. Larger width of the rocking diffraction curve for ADP + Glycine sample also can be due to higher inner stress in the crystal matrix with incorporated molecules of glycine. More details may be obtained from the study of high-resolution diffuse X-ray scattering measurements [19], which is not the main focus of the present investigation.

3.5. Dielectric measurements

The dielectric constant is one of the basic electrical properties of solids. Dielectric properties are correlated with electro optic property of the crystals [20], particularly when they are non-conducting in nature. Practically, the presence of a dielectric between the plates of condenser enhances the capacitance. Essentially, dielectric constant is the measure of how easily a material is polarized in an external electric field.

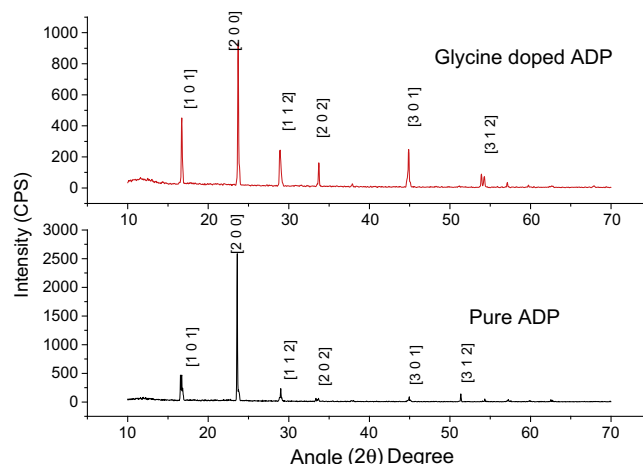


Fig. 5. Powder X-ray diffraction patterns of the grown crystals.

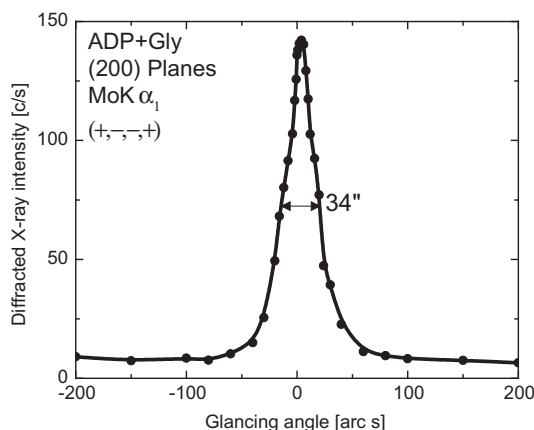


Fig. 6. High-resolution diffraction curves recorded for typical 1 mol% of glycine doped ADP single crystal.

Crystals with high transparency and large defect-free surface (i.e. without any pit or crack or scratch on the surface) grown by slow cooling method were used for the dielectric measurements. The dimensions of the crystals were $9 \times 9 \times 2 \text{ mm}^3$. Samples were coated with high quality grade silver paste in order to obtain the good conductive surface layer. The dielectric measurements were measured using Agilent 4284-A LCR meter. The capacitances of the crystals were measured using the conventional parallel plate capacitor method for frequency in the range 100 Hz to 1 MHz at different temperatures (not shown in the figure). The dielectric constant of the crystals were calculated using the relation:

$$\epsilon_r = C_{\text{crys}}/C_{\text{air}},$$

where C_{crys} is the capacitance of the crystal and C_{air} is the capacitance of same dimension of air. Fig. 7(a) shows the variation of dielectric constant of the pure and glycine added ADP with frequency 1 kHz at different temperatures. It is observed from the figure that the dielectric constant of the glycine added ADP increases with increase in temperature. This is the normal behaviour of the anti-ferroelectric nature of the ADP crystal. The same trend is observed in the case of variation of dielectric loss with frequency 1 kHz at different temperatures. The dielectric loss is less for the glycine added ADP. It is shown in Fig. 7(b). The electronic exchange of the number of ions in the crystals gives local displacement of electrons in the direction of the applied field, which in turn gives rise to polarization namely, electronic, ionic, dipolar and space charge polarization [21]. Space charge polarization is generally active at lower frequencies and high temperatures and indicates the perfection of the crystal. As the frequency increases, a point will be reached where the space charge cannot sustain and comply with the external field and hence the polarization decreases, giving rise to decrease in values of dielectric constant. The characteristic of high dielectric constant and low dielectric loss with high frequency for a given sample suggests that the sample possesses enhanced optical quality with lesser defects and this parameter is of vital importance for various nonlinear optical materials and their applications [13].

3.6. Vickers hardness

The good quality crystals are needed for various applications not only with good optical performance but also with good mechanical behaviour. Vickers hardness studies have been carried out using the instrument MITUTOYO model MH 120. The indentation hardness was measured as the ratio of applied load to the surface area of the indentation. The pure and doped crystals of size

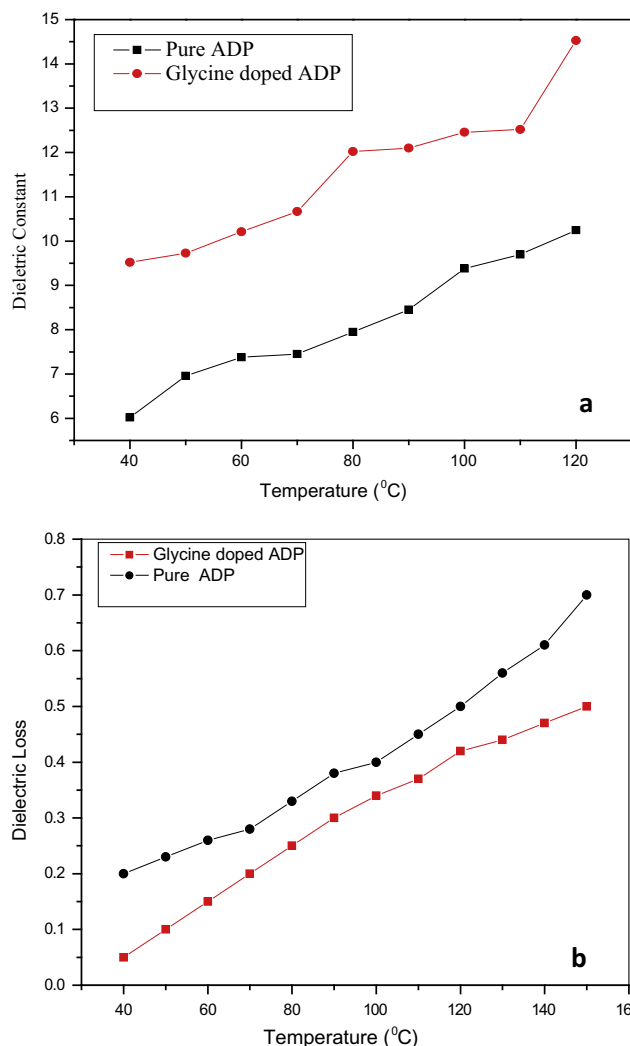


Fig. 7. Temperature dependence of (a) dielectric constant at 1 kHz and (b) dielectric loss at 1 kHz.

$5 \times 5 \times 3 \text{ mm}^3$ with (100) face was selected for microhardness studies. Indentations were carried out using Vickers indenter for varying loads. For each load (p), several indentations were made and the average value of the diagonal length (d) was used to

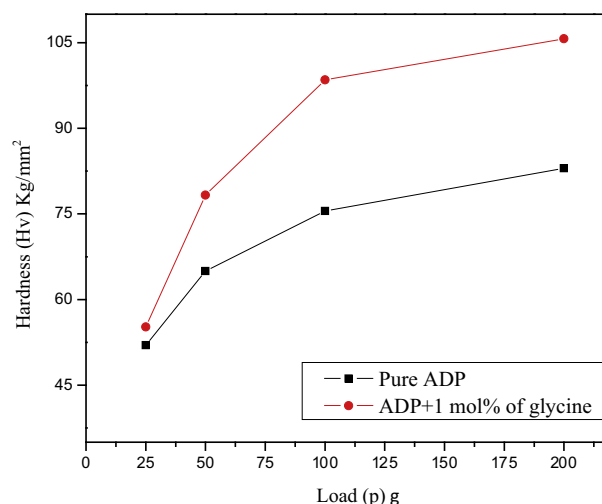


Fig. 8. Vickers microhardness of grown crystals.

calculate the microhardness of the crystals. Vickers microhardness number was determined using $H_v = 1.8544 p/d^2$ kg/mm². A plot drawn between the hardness value and corresponding loads is shown in Fig. 8. It is observed from the figure that hardness increases with increase in load for all the crystals and up to 100 g no cracks have been observed. Hardness is the resistance offered by a solid to the movement of dislocation. Practically, hardness is the resistance offered by a material to localized plastic deformation caused by scratching or by indentation. Due to the application of mechanical stress by the indenter, dislocations are generated locally at the region of the indentation. Higher hardness value for SR method grown crystal indicates that greater stress is required to form dislocation thus confirming greater crystalline perfection. Similar results were reported in ADP single crystals [22]. The ADP crystal has vacancy type of defects and they have been occupied by the doped glycine molecules and hence the crystalline perfection is improved. The improved crystalline perfection leads to the increase in the microhardness. Similar results have been observed in DL-Malic acid doped ADP and L-Lysine monochloride dihydrate ADP single crystals [23,24].

3.7. Thermal measurements

Thermal analysis was performed using Perkin–Elmer diamond TG/DTA instrument in nitrogen atmosphere. Fig. 9 shows the TG/DTA spectra for pure and doped ADP crystals. The DTA curve shows an endothermic peak at 215 °C for the pure ADP [23] and at 203 °C for the glycine doped ADP. It is observed from the figure that the decomposition temperature of the ADP is decreased by 12 °C. The measurement was repeated several times and same results were observed. The presence of glycine decreases the decomposition temperature of the ADP single crystals. Several experiments confirm that “the decomposition temperature of the parent material decreases if the decomposition temperature of the dopant is low compared to the parent material”. Our results appear to be in order Glycine molecule has lower decomposition temperature compared to ADP. Hence the presence of glycine decreases the decomposition temperature of the ADP single crystals. The same has been obtained in DL-Malic acid doped ADP and L-Lysine monochloride dihydrate ADP single crystals [23,24].

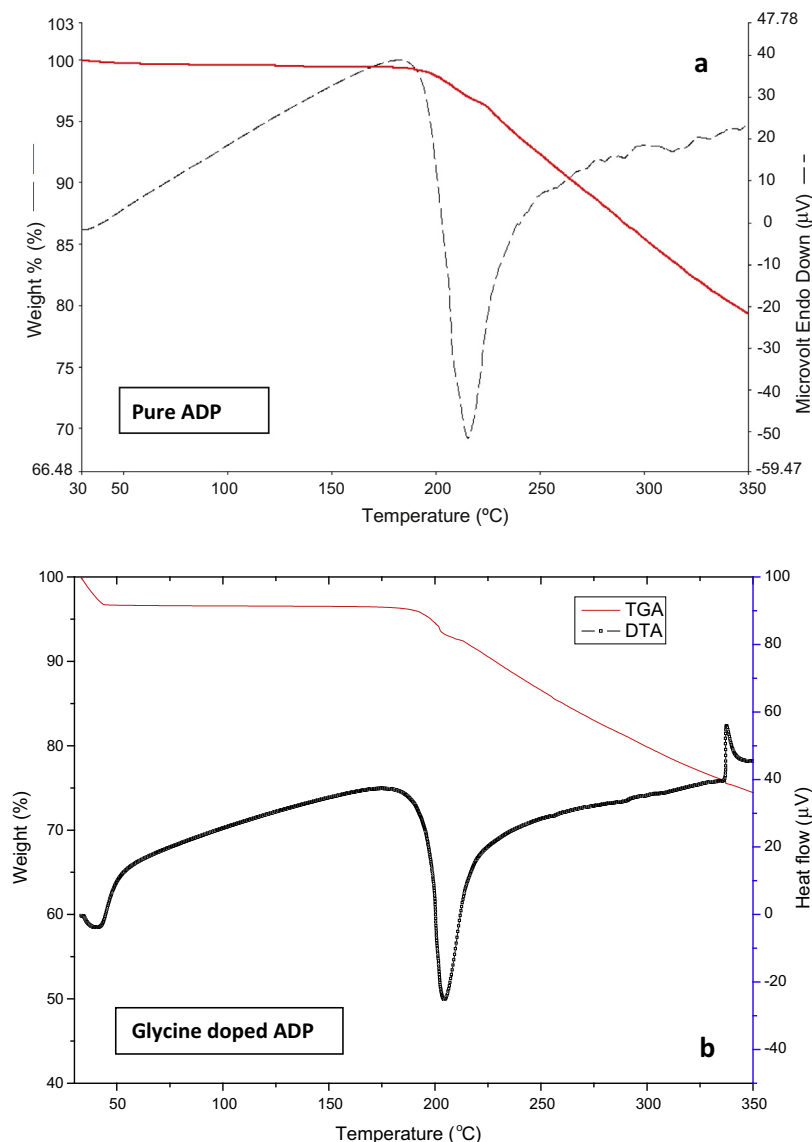


Fig. 9. TG–DTA curves of grown crystals.

3.8. Piezoelectric studies

A piezoelectric substance is one that produces an electric charge when a mechanical stress is applied. The piezoelectric property is related to the polarity of the material. C-cut plate of pure, glycine added ADP crystals were subjected to piezoelectric studies. The measurements were carried out for the grown crystals without poling the crystals. The obtained piezoelectric coefficient (d_{33}) value for pure ADP is 0.12 pC/N [24] and for the glycine doped crystal it is 0.171 pC/N. Higher piezoelectric coefficient has been obtained for the doped crystal. Higher crystalline perfection may be the reason for the same.

3.9. SHG efficiency

The powder sample was packed in a triangular cell and was kept in a cell holder. 1064 nm laser from Nd:YAG irradiates the sample. The monochromator was set at 532 nm. NLO signal was captured by the oscilloscope through the photomultiplier tube. The Nd:YAG laser source produces nanosecond pulses (8 ns) of 1064 nm light and the energy of the laser pulse was around 300 mJ. The beam emerging through the sample was focused on to a Czerny–Turner monochromator using a pair of lenses. The detection was carried out using a Hamamatsu R-928 photomultiplier tube. The signals were captured with an Agilent infinium digital storage oscilloscope interfaced to a computer. After the 4 averages, the signal height was measured (peak to peak volts). Similarly the signal height for the standard was also measured [22–24]. It is found that the SHG efficiency of the doped crystal is 0.5 time greater than pure ADP. The measured values are given in Table 1. It is necessary to mention here that the nonlinear and linear optical properties of the crystals are sensitive to the degree of intrinsic inter-molecular defects [25].

3.10. Laser damage threshold

The studies have been carried out for pure and doped ADP single crystals grown by slow cooling method using a Nd:YAG laser. Cut and polished samples with smooth and clear surface were chosen for the present study. Laser-induced surface damage threshold measurements were conducted using a high power Nd:YAG laser operating at 7 ns pulse width. Experiments were performed by keeping the positions of the lens and crystal plate as fixed and increasing the laser pulse energy until a visible spot was seen at the surface of the crystal. The crystal was placed at a distance where the beam diameter becomes 1.2 mm at the exit face of the crystal, the beam diameter was measured using knife edge measurements. In order to find the laser damage threshold, the used laser is nanosecond laser and in nanosecond lasers at low energies no self focusing is generated. For the LDT measurements laser beam was focused on the crystal with a 20 cm focal length convex lens and the crystal was placed just at the focal point. An attenuator was used to vary the energy of the laser pulses with a polarizer and a half wave plate. The pulse energy of each shot was measured by using combination of phototube

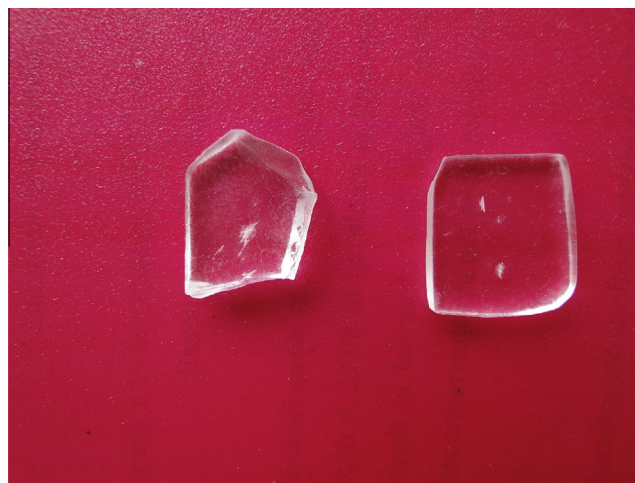


Fig. 10. Cracks obtained in the crystal during laser damage threshold studies (a) pure ADP and (b) glycine doped ADP.

and oscilloscope. In order to check the reproducibility the measurements have been repeated 3 times and the same results have been observed. During laser radiation, the power meter records the energy density of the input laser beam by which the crystal gets damaged. Two similar samples (similar in thickness and orientation) were prepared for laser damage threshold studies. The beam was passed along the (100) face for both crystals. The experiment started with the energy 5 mJ and continued in steps of 2 mJ and at 15 mJ damage was seen on the surface after 30 s. In the case of doped crystal, initially 10 mJ was applied and up to 30 s no crack was seen and the experiment was repeated by increasing the energy in steps of 2 mJ and at 22 mJ after 20 s a small dot was seen on the surface and finally a crack was seen when applying 24 mJ for 10 s. The observed cracks on the surface of the crystals are shown in Fig. 10. The laser damage threshold of glycine doped ADP crystal is high compared to the pure ADP. The higher crystalline perfection of the grown crystal may be responsible for high laser damage threshold.

Azarov et al. [26] reported that the damage threshold was influenced by the dislocation in the KDP crystal, and the crystal with many dislocations presented low damage threshold. On the other hand, Newkirk et al. [27] showed no direct relation between the dislocation in KDP crystals and the damage threshold. Nishida et al. [28] used KDP samples with few dislocations in which the organic impurities seemed to play a main role in causing bulk laser damage.

4. Conclusion

Optically transparent large size single crystals of glycine doped ADP was grown successfully using big crystal plate as seed and a point seed in minimum duration. The grown crystal is found mechanically harder than the pure ADP. Glycine doped crystals show higher intensity of green signals than pure ADP crystals because of having better optical quality. 20% of transparency has been increased compared to the pure ADP. It is concluded that the addition of glycine in the mother solution acts as a dopant and enhanced the growth rate and other properties of the crystals. This study will be helpful to grow high quality ADP crystals with good piezoelectric, laser damage threshold and SHG efficiency.

Table 1
SHG values of the grown crystals.

S. No.	Pure ADP (mV)	Glycine doped ADP (mV)
1	0.371	0.517
2	0.372	0.525
3	0.386	0.505
4	0.366	0.491

References

- [1] P. Rajesh, P. Ramasamy, G. Bhagavannarayana, *J. Cryst. Growth* 311 (2009) 4075.
- [2] S.M. Dharmapragash, P. Mohan Rao, *J. Mater. Sci. Lett.* 8 (1989) 1167.
- [3] Xu Dongli, Dongfeng Xue, *J. Cryst. Growth* 286 (2006) 108.
- [4] Xu Dongli, Dongfeng Xue, *J. Cryst. Growth* 310 (2008) 1385.
- [5] M.E. Lines, A.M. Glass, *Principles and Applications of Ferroelectrics and Related Materials*, Clarendon Press, Oxford, 1977.
- [6] N.G. Parsonage, L.A.K. Staveley, *Disorder in Crystals*, Clarendon Press, 1978.
- [7] N. Zaitseva, L. Carman, I. Smolsky, *J. Cryst. Growth* 241 (2002) 363.
- [8] L. Tenzer, B.C. Frazer, R. Pepinsky, *Acta Cryst.* 11 (1958) 505.
- [9] Yokotani, T. Sasaki, K. Yamanaka, C. Yamanaka, *Appl. Phys. Lett.* 48 (1986) 1030.
- [10] Yusuke Asakuma, Qin Li, H. Ming Ang, Moses Tade, Kouji Maeda, Keisuke Fukui, *Appl. Surf. Sci.* 254 (2008) 4524.
- [11] A. Cyrac Peter, M. Vimalan, P. Sagayaraj, J. Madhavan, *Physica B* 405 (2010) 65.
- [12] P. Rajesh, K. Boopathi, P. Ramasamy, *J. Cryst. Growth* 318 (2011) 751.
- [13] P. Rajesh, P. Ramasamy, *Physica B* 405 (2010) 1287.
- [14] P. Rajesh, P. Ramasamy, *Mater. Lett.* 63 (2009) 2260.
- [15] P. Rajesh, P. Ramasamy, *Mater. Lett.* 64 (2010) 798.
- [16] Yokotani, T. Sasaki, K. Yamanaka, C. Yamanaka, *Appl. Phys. Lett.* 48 (1986) 1030.
- [17] B.W. Batterman, H. Cole, *Rev. Mod. Phys.* 36 (1964) 681.
- [18] G. Bhagavannarayana, S. Parthiban, Subbiah Meenakshisundaram, *Cryst. Growth Des.* 8 (2008) 446.
- [19] Krishan Lal, G. Bhagavannarayana, *J. Appl. Cryst.* 22 (1989) 209.
- [20] S. Boomadevi, R. Dhanasekaran, *J. Cryst. Growth* 261 (2004) 70.
- [21] P. Rajesh, P. Ramasamy, C.K. Mahadevan, *J. Cryst. Growth* 311 (2009) 1156.
- [22] P. Rajesh, P. Ramasamy, *Physica B* 404 (2009) 1611.
- [23] P. Rajesh, P. Ramasamy, *J. Cryst. Growth* 311 (2009) 3491.
- [24] P. Rajesh, P. Ramasamy, C.K. Mahadevan, *Mater. Lett.* 64 (2010) 1140.
- [25] V. Krishnakumar, S. Manohar, R. Nagalakshmi, M. Piasecki, et al., *Eur. J. Appl. Phys.* 47 (2009) 30701.
- [26] C.V. Azarov, L.V. Atroshchenko, Yu.K. Danileiko, M.I. Kolybaevs, Yu.P. Minaev, V.N. Nikolaev, A.V. Sidorin, B.I. Zakharkin, *SoV. J. Quantum Electron.* 15 (1985) 89.
- [27] H. Newkirk, J. Swain, S. Stokowski, D. Milam, *J. Cryst. Growth* 65 (1983) 651.
- [28] Y. Nishida, T. Yokotani, T. Sasaki, K. Yoshida, T. Yamanaka, C. Yamanaka, *Appl. Phys. Lett.* 52 (1988) 420.